

The state of the art of explosive loads characterisation

AM Remennikov

University of Wollongong

Abstract

This paper presents the state of the art of characterisation of explosive loads of engineering structures. In recent years, high explosive devices have become the weapon of choice for the majority of terrorist attacks. Such factors as the accessibility of information on the construction of bomb devices, relative ease of manufacturing, mobility and portability, coupled with significant property damage and injuries, are responsible for significant increase in bomb attacks all over the world. In most of cases, structural damage and the glass hazard have been major contributors to death and injury for the targeted buildings. Following the events of September 11, 2001, the so-called “icon buildings” are perceived to be attractive targets for possible terrorist attacks. Research into methods for protecting civilian buildings against such bomb attacks has been initiated. Several analysis methods available to predict the loads from a high explosive blast on buildings in complex city geometries are examined. Analytical and numerical techniques are presented and the results obtained by different methods are compared. Results of the numerical simulations presented in this paper for multiple buildings in an urban environment have demonstrated the importance of accounting for adjacent structures when determining the blast loads on buildings.

Introduction

Protecting civilian buildings from the threat of terrorist activities is one of the most critical challenges for structural engineers today. Events of the past few years have greatly heightened the awareness of structural designers of the threat of terrorist attacks using explosive devices. Extensive research into blast effects analysis and techniques to protect buildings has been initiated in many countries to develop methods of protecting critical infrastructure and the built environment. The private sector is also increasingly considering measures to protect so-called “icon buildings” against the threat of external terrorist bomb attacks.

There are a number of means available to help prevent a successful terrorist attack on a building. One of the most effective measures consists of gathering intelligence that can be used to stop an attack before it takes place. Another measure that can be used to protect many new and existing buildings is the design and retrofit of structures, which can resist blast loadings and protect occupants. This area of research is currently receiving a great deal of attention by the engineering community.

What can be done to ensure structural integrity from explosive blasts with minimum loss of life or property? Structural engineers today need guidance on how to design structures to withstand various terrorist acts. While the issue of blast-hardening of structures has been an active topic with the military services, the relevant design documents are restricted to official use only. A very limited body of design documentation currently exists which can provide engineers with the technical data necessary to design civil structures for enhanced physical security. The professional skills required to provide blast resistant consulting services include structural dynamics, knowledge of the physical properties of explosive detonations and general knowledge of physical security practices.

Although it is recognised that no civilian buildings can be designed to withstand all conceivable terrorist threats, it is possible to improve the performance of structural systems by better understanding the factors that contribute to a structure's blast resistance. One such factor is the ability of the structural designer to accurately predict the blast loadings on structural components using analytical or numerical tools that take into account the complexity of the building, the presence of nearby structures and the surrounding environment.

Historical records indicate that the majority of terrorist incidents have occurred in an urban environment in the presence of nearby buildings forming the street geometries. Intuition suggests that the peak pressure and impulse associated with the blast wave should be higher in narrow streets, compared to wider ones. In fact, it has been observed that the confinement provided by tall buildings could drastically increase the blast loads by an order of magnitude or more above that produced in the free field by the same explosion source. However, systematic quantification of these effects has only recently been addressed by a few researchers [1-3], and they are still not described satisfactorily over a wide range of possible distances and street configurations.

The aim of this paper is to demonstrate the nature of explosions, analytical and computational approaches to determining the blast loads, and importance of considering the effects of congestion between buildings on blast loading.

Nature of explosions

An explosive is any chemical compound, mixture, or device, the primary purpose of which is to function by an explosion. Explosions are characterised as one of the three types: (1) mechanical; (2) nuclear; and (3) chemical. Chemical explosions are caused by extremely rapid conversion of a solid or liquid compound into hot gases having a much greater volume than the substances from which they are generated. It is the last type of explosion mentioned above that is used to manufacture a bomb for terrorist attacks.

Bare, solid explosives must detonate to produce any explosive effect other than a fire. The term detonation refers to a very rapid and stable chemical reaction, which proceeds through the explosive material at a speed, called the detonation velocity. Detonation velocities range from 5,000 to 8,000 metres per second for most high explosives. The detonation wave rapidly converts the solid or liquid explosive into a very hot, dense, high-pressure gas, and the volume of this gas, which had been the explosive material, is then the source of strong blast waves in air. Pressures immediately behind the detonation wave front range from 18,000 to 35,000 MPa. Only about one-third of the total chemical energy available in most high explosives is released in the detonation process. The remaining two-thirds is released more slowly in explosions in air as the detonation products mix with air and burn [4].

Explosives come in various forms, commonly called by names such as TNT, PETN, RDX, Semtex, and other trade names. A common explosive employed in rock blasting, called ANFO, consists of ammonium nitrate and fuel oil – products that are readily available. It is interesting to note that simple homemade devices fabricated by amateurs have proven just as destructive as more sophisticated commercial explosives. Terrorist organisations often manufacture their own explosive devices out of ordinary, commercially available materials – lawn fertiliser and diesel fuel. These materials are perfectly legal to possess until actually assembled into a bomb. In the quantities necessary to attack substantial structures, these materials behave as high explosive materials.

The use of trinitrotoluene (TNT) as a 'reference' explosive in blast-resistant design is universal. In order to quantify blast effects from a high explosive other than TNT, the actual mass of the charge has to be converted into a TNT equivalent mass by multiplying the mass of explosive by a conversion factor. Conversion factors represent the ratio of energy output of the explosive material to that of TNT and are given in Table 1 adapted from [5].

Table 1. Conversion factors for selected explosives

Explosive	TNT equivalent
TNT (trinitrotoluene)	1.000
RDX (Cyclonite)	1.185
PETN	1.282
Compound B (60% RDX 40% TNT)	1.148
Pentolite 50/50	1.129
Dynamite	1.300
Semtex	1.250

Characteristics of the blast wave

Most of the material damage caused by an explosion near the ground surface is due to the shock (or blast wave) which accompanies the explosion. Many structures will suffer some degree of damage from air blast when the overpressure in the blast wave (i.e. the excess over the atmospheric pressure 101 kPa at standard sea level condition) is about 3 – 5 kPa or more. The distance to which this overpressure level will extend depends primarily on the energy of the explosion. It is therefore important to consider the air blast phenomena associated with the passage of a blast wave through the air.

The expansion of the hot gases at extremely high pressures in the fireball causes a shock wave to form, moving outward at high velocity. This wave is characterised by a very sharp pressure rise at the moving front and rapid decrease in the pressure toward the interior region of the explosion. In the very early stages, the variation of the pressure with distance from the centre of the fireball is somewhat as shown in Figure 1 for an ideal shock front. As the blast wave travels away from the source, the overpressure at the front steadily decreases. After a short time, when the shock front has travelled a certain distance, the pressure behind the front drops below that of the surrounding atmosphere and a so-called “negative phase” of the blast wave forms. Figure 1 illustrates the overpressures at six successive times. In the curves marked t_1 through t_5 , the pressure in the blast is above atmospheric, but in the curve marked t_6 it is seen that at some distance behind the shock front the overpressure has a negative value. In this region the air pressure is below that of the ambient pressure so that an “underpressure” rather than an overpressure exists.

When an explosion occurs, a sudden release of energy to the atmosphere results in a pressure transient, or blast wave. The blast wave propagates radially in all directions from the source at supersonic speed. The magnitude and shape of the blast wave depends on the nature of the energy release as well as the distance from the point of explosion. Detonation of high explosives usually produces a characteristic shape known as an ideal blast wave (see Figure 2). The shock wave is characterised by an almost instantaneous rise in pressure from ambient atmospheric pressure P_0 to a *peak incident overpressure* P_{so} . The peak incident overpressure decays exponentially to the ambient value in time t_0 , which is the positive phase duration. This is followed by a negative pressure wave with a duration t_0^- that is usually much longer than the positive phase and is characterised by a maximum negative

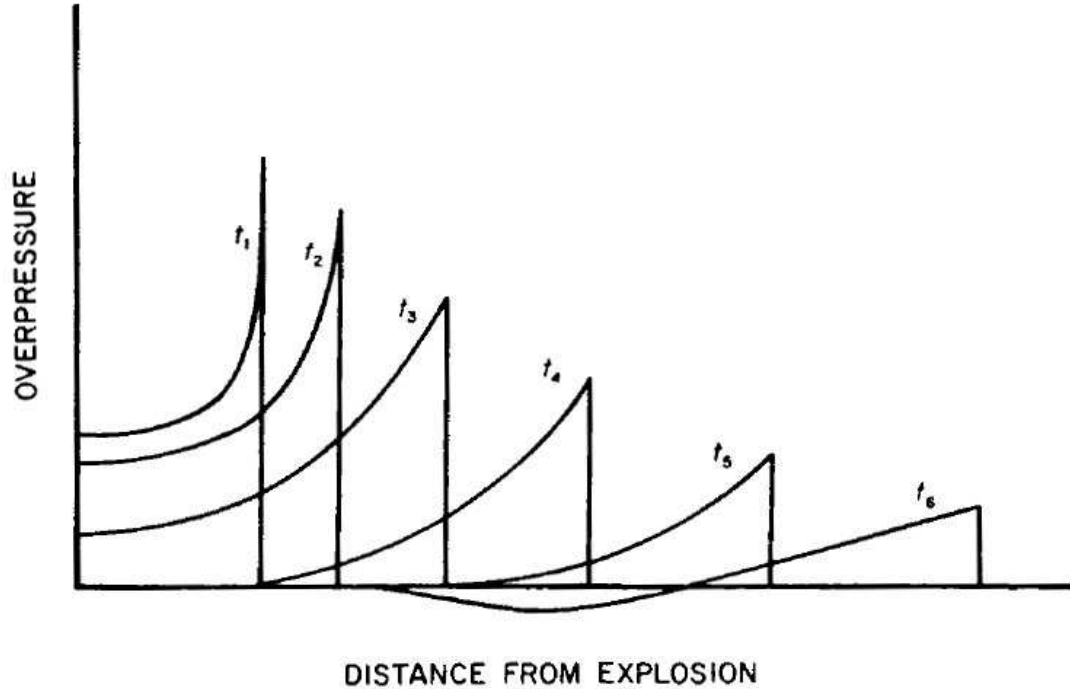


Figure 1: Variation of overpressure with distance

pressure P_s^- . These negative phase pressures subject buildings to blast loads acting in the direction opposite to that of the original shock. Because negative phase pressures are relatively small, and oppose the primary lateral force, it is usually conservative to ignore them in blast resistant design.

The impulse of the incident pressures associated with the blast wave is the integrated area under the pressure-time curve. Consequently, the positive phase impulse, i_s , is defined as follows:

$$\begin{aligned}
 i_s &= \int_{t_a}^{t_a+t_0} P(t) dt \\
 &= c P_{so} t_0
 \end{aligned} \tag{1}$$

where $P(t)$ represents the pressure - time relationship; P_{so} is the peak incident overpressure; t_0 is the duration of positive phase; t_a is the blast wave arrival time; and c is a value between 0.2 and 0.5 depending on the equation used to describe the variation of pressure with time $P(t)$.

As the blast wave propagates through the atmosphere, the air behind the shock front is moving outward at lower velocity. The velocity of the air particles, and hence the wind pressure, depends on the peak overpressure of the blast wave. This latter velocity of air is associated with the *dynamic (blast wind) pressure*, q . For typical conditions, standard relationships have been established between the peak incident pressure, P_{so} , the peak dynamic pressure, q_0 , the wind velocity, and the air density behind the shock front. These relationships state that the magnitude of the dynamic pressure, shock front velocity and air density are solely a function of the peak incident overpressure, and, hence, independent of the explosion size.

force is influenced primarily by such characteristics of the structure as the shape and size, but the drag force also depends on the peak value of the dynamic pressure and its duration. The dynamic pressure is proportional to the square of the wind velocity and to the density of the air behind the shock front. Some peak dynamic pressures and maximum blast wind velocities corresponding to various peak overpressures are given in Table 2.

Table 2. Peak overpressure, dynamic pressure and maximum wind velocity for an ideal shock front

Peak overpressure, kPa	Peak dynamic pressure, kPa	Maximum wind velocity, m/sec
1379	2275	929
1034	1531	794
690	848	633
496	510	522
345	283	417
207	117	299
138	56	224
69	15	131
34	4	73
14	1	31

It can be noted that for very strong shocks the peak dynamic pressure is larger than the peak overpressure, but below about 500 kPa overpressure the dynamic pressure is the smaller. Similar to the peak overpressure, the peak dynamic pressure decreases with increasing distance from the explosion centre, although the rate is different.

Nearly all the direct damage caused by both overpressure and dynamic pressure occurs during the positive overpressure phase of the blast wave. Although the dynamic pressure lasts for a longer time, its magnitude during this time is usually very low so that the associated destructive effects are not very significant. There may be some direct damage to structural elements during the negative phase of the blast wave; for example, large windows which are not properly secured against outward motion, brick veneer, and plaster walls may be dislodged by negative overpressures. The peak negative pressure is generally quite small in comparison with the positive peak pressures at the shock front; hence there is usually less damage caused during the negative phase of the blast wave.

Blast loading classification

According to Reference [4], blast loads on structures can be divided into two main groups based on the confinement of the explosive charge (unconfined and confined explosions) and can be subdivided based on the blast loading produced within the structure or acting on structures. These blast loading categories are illustrated in Table 3. Table 3 gives the six blast loading categories possible. Table 3 also shows the five possible pressure loads associated with the blast load categories.

Some of the blast loading categories relevant to this paper are qualitatively defined below and in the subsequent sections:

When an explosion occurs adjacent to and above a building structure such that no amplification of the initial shock wave occurs between the explosive charge and the structure, then the blast loads on the structure are *free-air* blast pressures.

The *air burst* environment is produced by explosions that occur above the ground surface and at a distance away from the building structure so that the initial shock wave, propagating away from the explosion, impinges on the ground surface prior to arrival at the structure.

If a charge is located on or very near the ground surface, the blast environment is considered to be a *surface burst*. The initial wave of the explosion is reflected and reinforced by the ground surface to produce a reflected wave.

Table 3. Blast loading categories [4]

Blast Loading Categories		
Charge Confinement	Category	Pressure Loads
Unconfined explosions	1. Free Air Burst	a. Unreflected
	2. Air Burst	b. Reflected
	3. Surface Burst	b. Reflected
Confined explosions	4. Fully Vented	c. Internal shock
		d. Leakage
	5. Partially Confined	c. Internal shock
		e. Internal gas
		d. Leakage
	6. Fully Confined	c. Internal shock
e. Internal gas		

Reflection of blast wave at a surface

When the incident blast wave strikes a rigid surface such as the ground surface or a front wall of a building, it is reflected. The formation of the reflected wave in an air burst is shown in Figure 3. This figure shows four stages in the outward motion of the spherical blast wave originating from an air burst. In the first stage the wave front has not reached the ground; the second stage is somewhat later in time, and in the third stage a reflected wave, indicated by the dashed line, has been produced.

The exact value of the peak reflected pressure will depend on the strength of the incident wave and the angle of incidence. The nature of the surface also has an important effect, but it is usually assumed to be smooth (or ideal) so it acts as an ideal reflector. The variation in overpressure in time, as observed at a point on the surface not too far from the centre of explosion (e.g. point A in Figure 3) is similar to the one depicted in Figure 2 for an ideal shock front. The point A may be considered as lying within the region of “regular” reflection, i.e., where the incident and reflected waves do not merge except on the surface.

At any point somewhat above the ground surface, two separate shocks will be recorded, the first being due to the incident blast wave and the second to the wave reflected off the ground, which arrives a short time later. This situation can be illustrated by considering the point B in Figure 3. When the incident blast wave front reaches this point, at time t_3 , the reflected wave is still some distance away. After a short interval, the reflected wave reaches the point B at time t_4 . Between time instances t_3 and t_4 , the reflected wave has spread out to some extent, so that its peak overpressure will be less than the value at surface level.

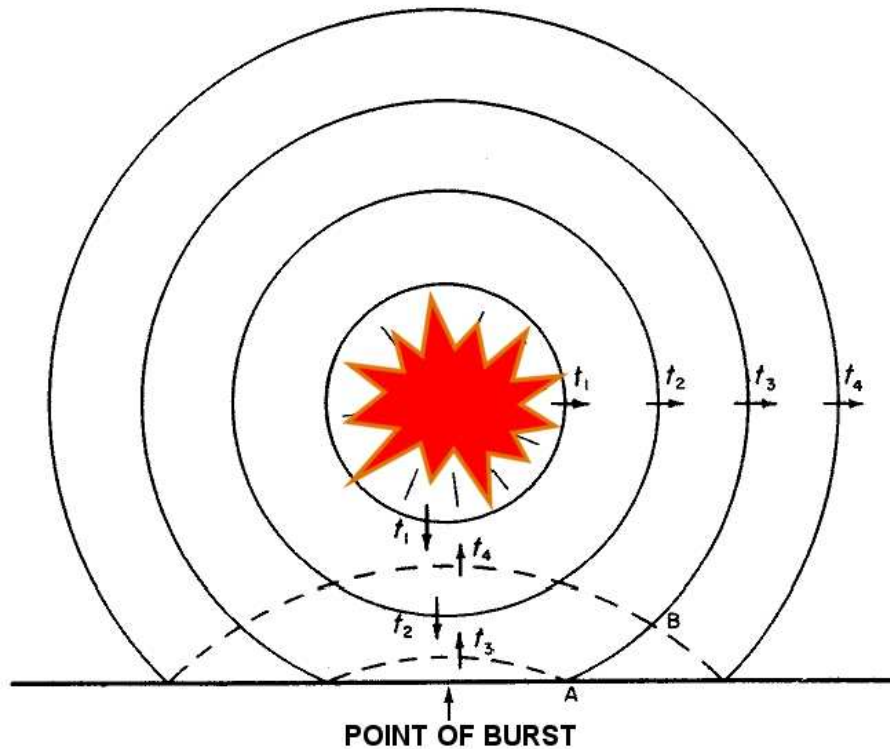


Figure 3: Reflection of blast wave at the ground surface for explosion occurring at some distance above ground

The above discussion concerning the delay between the arrival of the incident and reflected wave fronts at a point above the surface is based on the assumption that the two waves travel with approximately equal velocities. This assumption can be justified in the early stages of blast wave formation, when the wave front is reasonably close to centre of burst. However, it will be evident that the reflected wave always travels through air that has been heated and compressed by the passage of the preceding incident wave. As a result, the reflected wave front moves faster than the incident wave, and eventually overtakes it so that the two wave fronts merge to produce a single shock front. The process is called “Mach” or “irregular” reflection. Consequently, the region in which the two waves have merged is called the Mach or irregular region.

The merging of the incident and reflected waves is shown schematically in Figure 4. It can be seen that in the early stages the incident and reflected wave do not merge and the regular reflections take place. At a later stage, the steeper front of the reflected wave shows that it is travelling faster than the incident wave. This results in that the reflected wave overtakes the incident wave at some stage. After the reflected wave has overtaken and merged with the incident wave, a single shock front is formed called the “Mach stem.” The point at which the incident wave, reflected wave, and Mach fronts meet is referred to as the “triple point.”

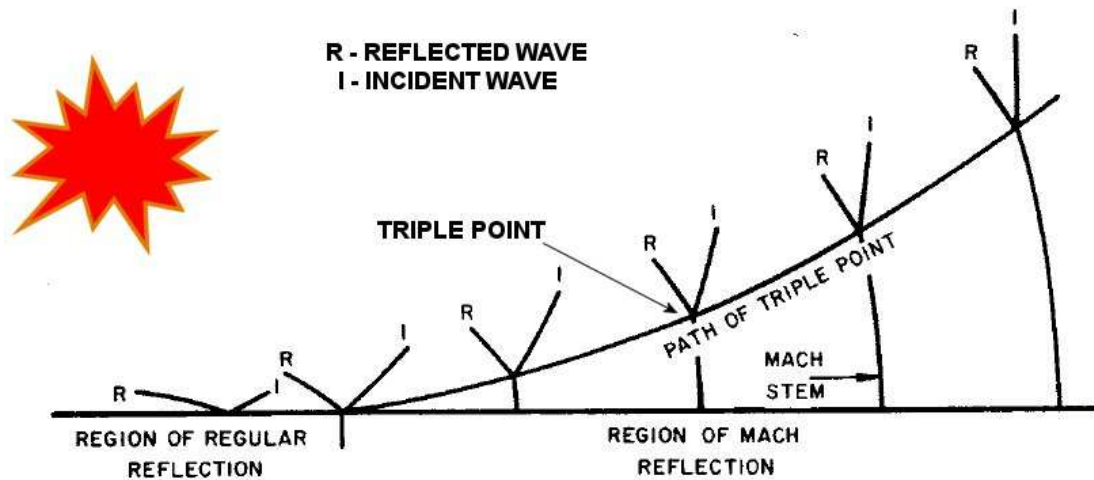


Figure 4: Merging of incident and reflected waves and formation of Mach front

As the reflected wave continues to overtake the incident wave, the triple point rises and the height of the Mach stem increases (Figure 4). Any object located either at or above the ground, within the Mach region and below the triple point path, will experience a single shock. The behaviour of the merged (Mach) wave is the same as that previously described for blast waves in general.

At points in the air above the triple point path, such as at the top of a high-rise building, two pressure pulses will be recorded. The first will be due to the incident blast wave and the second, a short time later, to the reflected wave. When a bomb is detonated at the surface, only a single merged wave develops. Consequently, only one pressure increase will be observed either on or above the ground.

The distance from point of burst at which the Mach stem begins to form depends upon the yield of detonation and the height of the burst above the ground. For moderate heights of burst, Mach merging of incident and reflected waves occurs at a distance from centre of explosion approximately equal to the burst height. As the height of burst is becoming greater, the distance at which the Mach stem forms exceeds the height of burst by larger and larger amounts.

Surface burst is somewhat different from an air burst described above. In a surface explosion the incident and reflected shock waves merge instantly, as seen in Figure 5. All objects on the surface are subjected to airblast similar to that in the Mach region below the triple point for an air burst. For an ideal (absolutely rigid) reflecting surface the shock wave characteristics, i.e., overpressure, dynamic pressure, etc., at the shock front would correspond to that for a “free air” burst, i.e. in the absence of a surface, with twice the weapon energy yield. Because of the immediate merging of the incident and reflected blast waves, there will be a single shock front which is hemispherical in form, as shown at successive times t_1 through t_4 in Figure 5. Near the surface, the shock front is essentially vertical and the dynamic wind behind the front will blow in a horizontal direction.

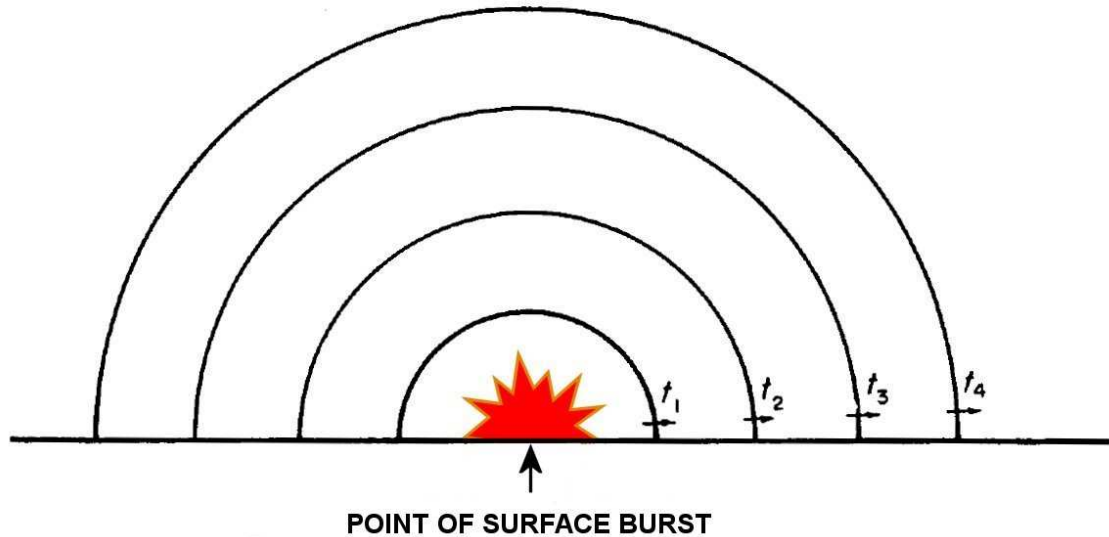


Figure 5: Blast wave from a surface burst

Due to their sudden application, high intensity and relatively short duration, loads produced by overpressure and dynamic pressure are generally more critical than the loads of a similar type, e.g. wind load, applied statically to the structure. The damaging effects of the even higher reflected pressures are reduced by their very short duration. Thus, the combination of the blast pressures causes heavy transient loads on structures stipulating the requirement for dynamic analysis to be considered in the structural design.

Peak blast loads may be several orders of magnitude larger than the largest loads for which conventional buildings are designed. For a hemispherical charge of 1000 kg of TNT, the peak pressure of the shock front at a distance of 5 m from the point of detonation is about 5,000 kPa (this overpressure will decay to ambient atmospheric pressure in about 2.5 msec); from a 2000 kg hemispherical charge, about 7,000 kPa. By contrast, a good wind gust might result in a pressure of 2 kPa on the surface of a building. The peak load resulting from the explosive detonation is about 2,500 times greater! At the same time, it should be emphasised that the blast load duration is extremely short compared to a wind gust. This fact stipulates the need to calculate the structural response to blast loading as a function of both the load magnitude and duration.

The peak pressure drops off rapidly with distance. For example, for a 1000 kg charge of TNT, a peak pressure of 2 kPa at the shock front is produced at about 400 m from the detonation point.

It is customary to characterise the pressure loadings in terms of scaled range, as given by $Z = R/W^{1/3}$, in which Z is the scaled range, R is the radial distance between the explosion centre and the target, and W is the explosive weight (normally expressed as an equivalent TNT weight). In the scaled-range concept, as long as the value of Z remains the same, the same parameters of explosive effects (i.e., peak pressures, scaled load duration) should be obtained. It should be noted that it is not possible to match both peak pressure and impulse from the scaled distance – only one unique charge weight and distance combination will produce any particular combination of pressure and impulse.

If a large-scale blast wave interacts with a structure, subjecting a large area of the structure to blast loading, then the structure will be loaded in a manner that leads to global deformation. In that case, all the elements provide some degree of resistance to the dynamic loading. If a relatively small charge is detonated sufficiently close to a substantial structure, the response

of individual elements needs to be considered separately since they are likely to be loaded sequentially. If the explosion is in close proximity to a wall or floor slab, there can be gross disintegration, with either spalled fragments coming off the front and back sides, or wall fragments themselves being propelled as missiles. These fragments can injure people, damage property and, if structural support is sufficiently damaged, cause the building to collapse. One example of such blast wave-structure interaction can be an abrupt removal of a principal exterior reinforced concrete column by the brisant effects in the Oklahoma City bombing in 1995. At intermediate scaled ranges, both global and localised responses can be expected resulting in severe cracking, with near-face disintegration and spalling of the rear face.

Methods to predict blast loads

The following methods are available for prediction of blast effects on building structures:

empirical (or analytical) methods;

semi-empirical methods;

numerical (or first-principle) methods.

Empirical methods are essentially correlations with experimental data. Most of these approaches are limited by the extent of the underlying experimental database. The accuracy of all empirical equations diminishes as the explosive event becomes increasingly near field.

Semi-empirical methods are based on simplified models of physical phenomena. They attempt to model the underlying important physical processes in a simplified way. These methods rely on extensive data and case study. Their predictive accuracy is generally better than that provided by the empirical methods.

Numerical (or first-principle) methods are based on mathematical equations that describe the basic laws of physics governing a problem. These principles include conservation of mass, momentum, and energy. In addition, the physical behaviour of materials is described by constitutive relationships. These models are commonly termed computational fluid dynamics (CFD) models.

Empirical methods

The empirical methods presented in this paper are mainly based on US Army Technical Manuals:

TM 5-1300 [4]

This manual is one of the most widely used publications available to both military and civilian sectors for designing structures to provide protection against the blast effects of an explosion. It contains step-by-step analysis and design procedures, including information on (i) blast loading; (ii) principles of non-linear dynamic analysis; and (iii) reinforced concrete and structural steel design.

The design curves presented in the manual give the blast wave parameters as a function of scaled distance for three burst environments: (i) free air burst; (ii) air burst; and (iii) surface burst.

When an explosion occurs adjacent to and above a building structure such that no amplification of the initial shock wave occurs between the explosive charge and the structure, then the blast loads on the structure are *free-air* blast pressures.

A scaling chart that gives the positive phase blast wave parameters for a surface burst of a hemispherical TNT charge is presented in Figure 6. Such scaling charts provide blast load data at a distance R (called the standoff distance) along the ground from a specific explosive. To compute blast loads at points above the ground, a simplified approach is presented later in this paper.

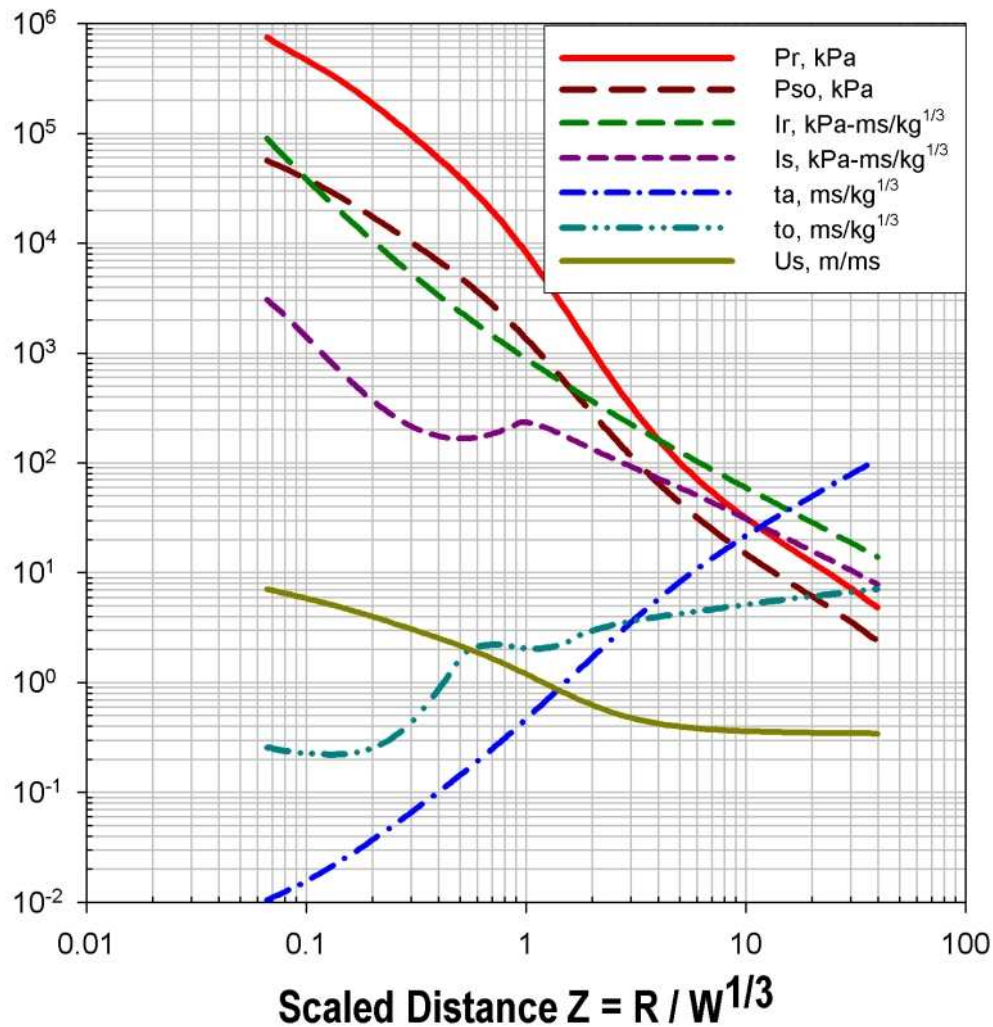


Figure 6: Positive phase shock wave parameters for TNT explosions at sea level [4].

The following step-by-step procedure for determining blast wave parameters for a surface blast is outlined in TM5-1300:

Step 1. Determine the charge weight, W , kilograms, as TNT equivalent, and ground distance R_G (m) from the charge to the surface of a structure.

Step 2. Calculate scaled ground distance, Z_G :

$$Z_G = R_G / W^{1/3} \text{ (Units: m/kg}^{1/3}\text{)}$$

Step 3. Read the blast wave parameters from Figure 6 for corresponding scaled ground distance, Z_G . To obtain the absolute values of the blast wave parameters, multiply the scaled values by a factor $W^{1/3}$.

For example, detonation of a 100-kg TNT hemispherical charge at a distance of 15m from a building will produce loading on the front wall with the following parameters:

$$\text{Scaled range } Z_G = 15 / (100)^{1/3} = 3.2 \text{ m/kg}^{1/3}$$

$$\text{Peak reflected overpressure } P_r = 272 \text{ kPa}$$

$$\text{Reflected impulse } i_r = 206 \times (100)^{1/3} = 956 \text{ kPa-msec}$$

$$\text{Time of arrival } t_a = 4.0 \times (100)^{1/3} = 18.6 \text{ msec.}$$

TM5-855-1 [6]

This manual provides procedures for the design and analysis of protective structures subjected to the effects of conventional weapons. It is intended for structural engineers involved in designing hardened facilities. It includes chapters on airblast effects, blast loads on structures, and auxiliary systems (air ducting, piping, etc). The manual also provides closed-form equations to generate the predicted airblast pressure – time histories.

This manual can also be used to evaluate blast loading on multi-storey buildings. Load time histories for buildings and building components located at some height above the ground can be calculated according to the methodology presented in TM5-855-1. The basic steps are outlined below:

Divide a surface into sub-sections and evaluate a pressure – time history and impulse for each small zone.

The total impulse applied to the surface is then obtained by summing up the impulses for each sub-section.

The total load – time history is then defined to have an exponential form with a peak calculated assuming an average peak pressure applied over all the surfaces.

One of the limitations of this simplified method lies in neglecting the true physics of the blast wave – structure interaction phenomena in that it assumes the load – time history is applied to all parts of the surface at the same time. This assumption provides a poor approximation for close-in blast effects.

To overcome the above limitation, another algorithm has been developed in which the total load on a surface at a particular time is computed by summing up the load on each sub-surface at that time. Thus, the calculation predicts a load – time history that has the same total impulse as estimated by the TM5-855-1 procedure above, but with a different load versus time relationship.

CONWEP Airblast Loading Model [7]

Kingery and Bulmash [8], also working for the US Army, have developed equations to predict airblast parameters from spherical air bursts and from hemispherical surface bursts. These equations are widely accepted as engineering predictions for determining free-field pressures and loads on structures. The Kingery-Bulmash equations have been automated in the computer program CONWEP [7].

Their report [8] contains a compilation of data from explosive tests using charge weights from less than 1kg to over 400,000kg. The authors used curve-fitting techniques to represent the data with high-order polynomial equations, which are used by CONWEP program. These equations can also be found in TM5-855-1 in graphical form only.

Unlike TM5-855-1, where an approximate equivalent triangular pulse is proposed to represent the decay of the incident and reflected pressure, CONWEP takes a more realistic approach, assuming an exponential decay of the pressure with time:

$$P(t) = P_{so} \left[1 - \frac{t - T_a}{T_0} \right] \exp \left[\frac{-A \times (t - T_a)}{T_0} \right] \quad (2)$$

where $P(t)$ is the pressure at time t (kPa); P_{so} is the peak incident pressure (kPa); T_0 is the positive phase duration (msec); A is the decay coefficient (dimensionless); and T_a is the arrival time (msec).

The above equation is usually referred to as the Friedlander equation. The airblast parameters in Equation (2) (peak incident and reflected pressure and impulse, positive phase duration, and time of arrival) are calculated using the equations found in [8]. Using the peak pressure,

impulse, and duration, the program iterates to find the decay coefficient A , which is dimensionless. The program then uses the Friedlander's equation (2) to find blast pressure values at various time steps.

Alternatively, tables of pre-determined shock wave parameters may be used to estimate blast pressure and impulse. As discussed previously, if a shock wave impinges on a rigid surface, a reflected pressure is instantly developed on the surface, and the pressure is raised to a value in excess of the incident pressure as illustrated in Figure 7.

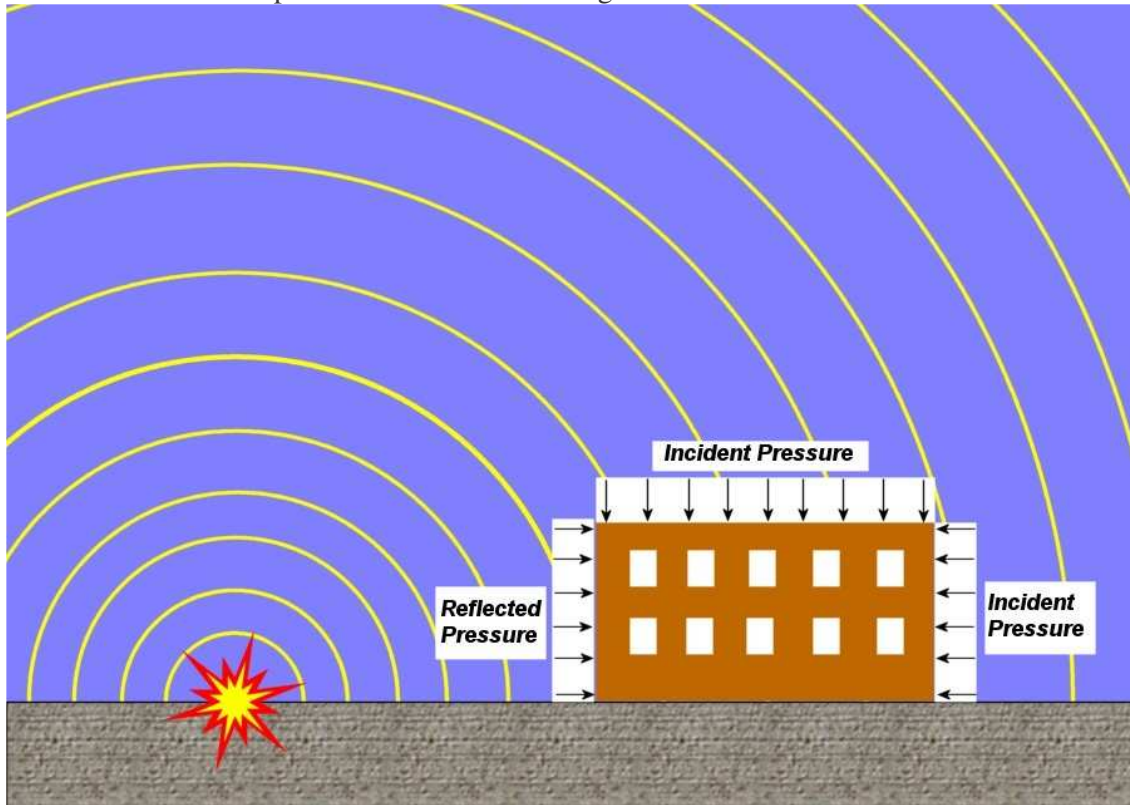


Figure 7: Incident and reflected pressures on building

Tables 4 through 7 provide airblast parameters for 25, 50, 250 and 500 kg TNT explosive charges at various standoff distances. These charges are the typical charge sizes for different explosive delivery methods ranging from a small hand-delivered bomb to a moving vehicle laden with high explosives.

Table 4. Airblast parameters for 25-kg TNT explosive charge

25-kg TNT	5m	15m	25m	50m	75m	100m
Peak reflected pressure (kPa)	1,700	95.8	39.8	15.2	9.0	9.2
Reflected impulse (kPa-msec)	1,291	357.0	205.0	98.7	64.7	47.8
Peak incident pressure (kPa)	407.3	41.3	18.5	7.4	4.4	3.0
Incident impulse (kPa-msec)	453.0	169.3	105.4	53.7	36.0	26.8

Table 5. Airblast parameters for 50-kg TNT explosive charge

<i>50-kg TNT</i>	<i>5m</i>	<i>15m</i>	<i>25m</i>	<i>50m</i>	<i>75m</i>	<i>100m</i>
<i>Peak reflected pressure (kPa)</i>	3,414	155.9	57.6	20.6	12.1	11.6
<i>Reflected impulse (kPa-msec)</i>	2,180	582.2	331.1	158.4	103.7	76.8
<i>Peak incident pressure (kPa)</i>	692.4	62.8	26.1	9.9	5.9	4.1
<i>Incident impulse (kPa-msec)</i>	705.8	261.4	165.2	84.8	57.1	42.9

Table 6. Airblast parameters for 250-kg TNT explosive charge

<i>250-kg TNT</i>	<i>5m</i>	<i>15m</i>	<i>25m</i>	<i>50m</i>	<i>75m</i>	<i>100m</i>
<i>Peak reflected pressure (kPa)</i>	14,708	631.0	165.3	44.7	24.6	19.8
<i>Reflected impulse (kPa-msec)</i>	7,653	1,857	1,025	478.2	310.9	230.0
<i>Peak incident pressure (kPa)</i>	2,170	191.3	65.9	20.6	11.7	8.1
<i>Incident impulse (kPa-msec)</i>	1,260	715.9	457.1	243.7	164.8	124.5

Table 7. Airblast parameters for 500-kg TNT explosive charge

<i>500-kg TNT</i>	<i>5m</i>	<i>15m</i>	<i>25m</i>	<i>50m</i>	<i>75m</i>	<i>100m</i>
<i>Peak reflected pressure (kPa)</i>	24,823	1,255	291.1	65.5	34.3	24.8
<i>Reflected impulse (kPa-msec)</i>	13,386	3,097	1,683	773.4	500.2	369.1
<i>Peak incident pressure (kPa)</i>	3,320	323.4	104.5	29.4	16.0	10.9
<i>Incident impulse (kPa-msec)</i>	1,380	1,118	703.5	381.4	259.8	196.5

Computing blast loads on a building at points above ground

A simplified geometry of a typical bomb threat on an office block is depicted in Figure 8. The blast loads on the vertical exterior wall of a building are calculated based on the input equivalent TNT charge weight (W), the charge location relative to the building, and the assumption of a relevant blast wave propagation model. There are generally two blast environments that could be considered in this situation: (1) a spherical air blast; and (2) a hemispherical surface blast.

Nearly all exterior bomb threats on architectural targets can be modelled using the surface burst model. In this model, a charge is located on or very near the ground surface. The wave of the explosion is reflected from the ground and reinforces the energy of the blast wave propagating through the air. If the ground were a perfectly rigid surface, approximately half of the bomb energy would be reflected from the ground effectively doubling the blast wave intensity. Since the ground is not a perfect reflector, some energy (about 20%) is lost in forming a crater and producing ground shock.

In Figure 8, the ground standoff distance, R_G , is calculated as the shortest distance from the centre of explosive charge to the exterior wall (or, the length of direct vector from the explosive charge which is normal to the surface). The standoff distance at height h , R_h , is introduced as the straight-line distance from the charge to the geometric centre of the area of interest, which is at height h above ground. The point of interest is always assumed to be at

the centre of the building component and the blast load at the centre is used as a uniform load over the entire structural component.

Effect of angle of incidence

According to the simplified procedure, the blast pressure on a vertical exterior wall will always be the fully reflected pressure corresponding to the calculated scaled standoff distance. One can argue that the simplified procedure does not consider the relationship between *angle of incidence* and reflection of the blast wave. The angle of incidence of a point on a surface is the angle between the outward normal and the direct vector from the explosive charge to the point. This is illustrated in Figure 8. It is well known that the angle of incidence is one of the factors, which generally affects the blast load on structural components.

For a given scaled standoff, $Z = R/W^{1/3}$, the pressure measured on a large rigid surface and an angle of incidence equal to zero degrees ($\alpha = 0$) is the fully reflected pressure P_r at that scaled standoff. For a given standoff, the pressure measured at a point on a surface that has an angle of incidence of 90 degrees (i.e., it is parallel to the direction of blast wave propagation) is the incident or side-on pressure P_{so} at the given scaled standoff distance. The impulse applied to a surface being the integral of the pressure – time history is also affected by the angle of incidence. The impulse is generally increased from its free-field value if the angle of incidence is less than 90 degrees.

If the angle of incidence is less than 45 degrees, use of fully reflected peak pressure and impulse can be justified by analysing the reflected pressure – angle of incidence relationship shown in Figure 9.

In Figure 9, the reflected peak pressure is the product of the side-on pressure and the reflection factor shown on the vertical axis of the figure. Only curves corresponding to peak side-on pressures less than or equal to 350 kPa are shown. Analysis of curves in Figure 9 indicates that, for the applicable side-on pressure levels, the peak blast pressure remains close to its full reflected value for angles of incidence less than approximately 45 degrees. Therefore, the assumption that the blast pressure remains constant at its full reflected value for small angles of incidence (less than 45 degrees) represents a good simplifying approximation.

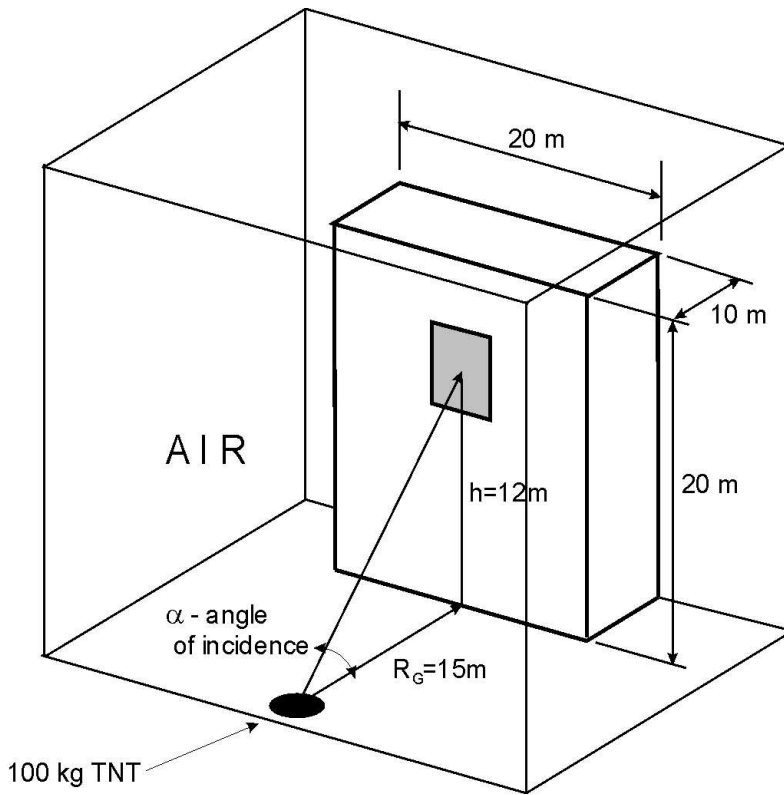


Figure 8: Geometry of a bomb threat on an office block

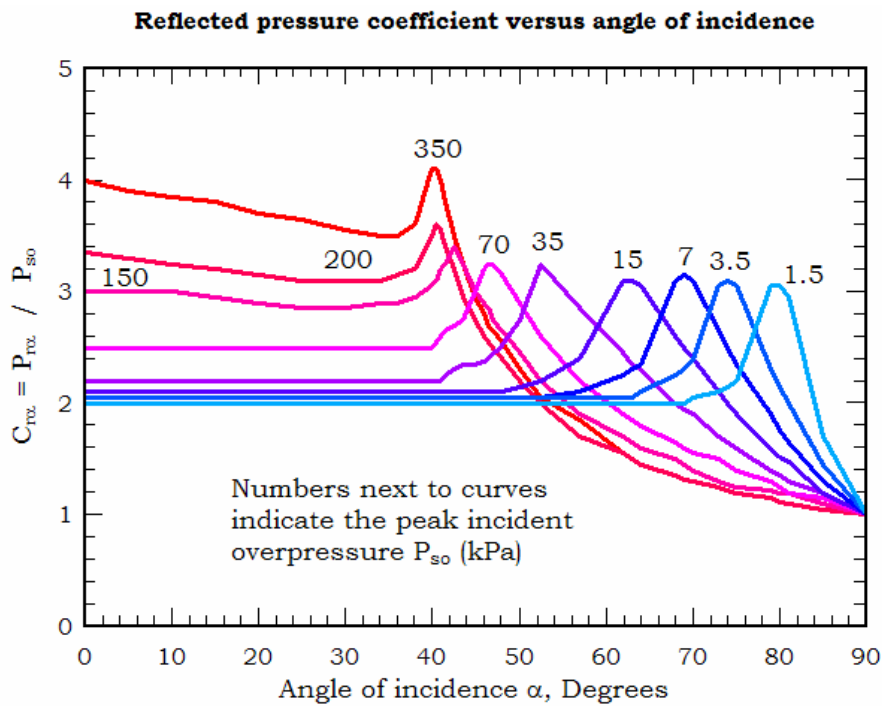


Figure 9: Reflected pressure vs. angle of incidence [4].

Impulse on the area of interest of the building surface with angles of incidence between zero and 45 degrees are predicted well with this simplified procedure (within 20% on the conservative side). For angles of incidence greater than 45 degrees, impulse on components can be underestimated by factors from 2.5 to 1.5 for angles of incidence between 45 and 70 degrees (see Figure 2-194 [4]).

For many buildings at larger standoffs from the explosive charge, most of the exterior wall components subjected to reflected pressures would be at angles of incidence less than 45 degrees. This fact renders the simplified procedure for computing blast loads at points above ground to be well suited for engineering calculations of blast induced effects on commercial buildings.

Procedure:

Step 1. Determine the explosive charge weight, W . Assume a hemispherical surface burst model. Select point of interest (centre of area) on the exterior vertical wall of a building at height h above ground.

Step 2. For the point of interest, calculate standoff distance at height h , R_h , scaled standoff distance, Z_h , and angle of incidence, α :

$$R_h = (R_G^2 + h^2)^{1/2}$$

$$Z_h = R_h / W^{1/3}$$

$$\alpha = \tan^{-1}(h/R_G)$$

Step 3. From Figure 6 read peak reflected pressure P_r and scaled positive reflected impulse $i_r/W^{1/3}$. Multiply scaled impulse by $W^{1/3}$ to obtain absolute value.

Numerical simulation of blast loads on multiple buildings

Several experimental and numerical studies [1,3,9] have demonstrated that the blast loads on a building are affected by the presence of adjacent structures. Whether the blast loads are reduced due to shadowing by other buildings or augmented due to reflection and channelling of the airblast pressure is generally determined by the design of the buildings, the layout of nearby streets, and the location and size of the explosive device.

A limited number of experiments involving small-scale models have been conducted to validate numerical simulations of blast wave – multiple structures interaction [9]. A combined experimental–analytical approach has proven to be the most economical way to investigate the phenomenology of blast wave propagation in complex city terrains. Numerical simulations can be used to extend the database of blast effects in urban terrains by varying the parameters in numerical models. Moreover, analyses can be performed for cases where experiments cannot be performed or where the required design information cannot be extracted from experimental results. Based on the results of the simulations, validated and improved methods can be developed for predicting blast loads on buildings in congested city environments.

To better understand the phenomenology that affects the blast loads on a structure, numerical simulations were performed using the Australian Partnership for Advanced Computing (APAC) High Performance Computing (HPC) facilities. The computer code Air3D [10], which is specifically designed for shock and blast simulations and is compiled to run on the supercomputer, was used to perform a series of airblast calculations in this paper.

The buildings are typically modelled as rigid reflective surfaces in Air3D. Typical simulation of blast wave – rigid building interaction with Air3D includes three stages with automatic remapping between each stage: (1) one-dimensional analysis for the spherically symmetrical region between the centre of the explosive charge and the ground, if the high explosive (HE) source is detonated above the ground level; (2) two-dimensional blast wave propagation for the radially symmetrical region from the time when the blast wave reaches the ground level to

when it reaches the nearest surface of the target building; and (3) three-dimensional analysis to capture such effects as multiple reflection, diffraction, blast focusing and shielding. The modelled space in Air3D should be extended sufficiently far in each direction so that the presence of the boundaries does not affect the solution. The practical way to verify this is to move the boundaries inwards until the results at the measuring locations become significantly affected. All the models presented in this paper included this numerical test in order to validate the positions of the boundaries.

Mesh refinement studies should also be performed for CFD calculations. For the numerical simulations presented in this paper, a mesh refinement study was performed using a three-dimensional model. An initial analysis was performed using constant cell spacing equal to four times the minimum cell size. The minimum cell size is usually influenced by the computational resources and compute time available and not always the same as the optimum cell size. Four 3-D analyses were performed for each model using 1.0, 0.5, 0.333, and 0.25 times the coarsest cell size. By comparing pressures and impulses for several key locations on the building, convergence of the solution can be verified.

Sometimes an indication of the numerical accuracy of the solutions obtained for the full model can also be obtained by comparing the blast load simulation results with the free-field airblast predictions using widely accepted and validated empirical relationships [7] for the locations not affected by diffraction, multiple reflections or confinement effects.

Shielding effects and reflection of pressure off the adjacent structures were studied in the two-building simulation. Two target buildings and the geometric parameters of the model are shown in Figure 10. The two-building model represents a scenario where the explosive charge of W kg of TNT equivalent is detonated at close range from a smaller building (Building 1) that provides partial shielding to an adjacent larger building (Building 2). The scaled standoff distance to Building 1 is $Z_1 = R_1/W^{1/3} = 0.5 \text{ m/kg}^{1/3}$, and the standoff distance to Building 2 is $Z_2 = 2.0 \text{ m/kg}^{1/3}$. The height of the buildings was also scaled by the cube root of the explosive weight, W , in order to be used as the design parameter. In the model, the centre of the explosive charge was in line with the centres of the target buildings.

The two-building model comprised about $5,000,000 \times 10$ mm cubic cells with the cell size established as a result of the mesh refinement studies described earlier. The three-dimensional model was extended in each direction so that the presence of boundaries did not affect the results of analyses. The target points, where blast pressure and impulses were measured, were distributed over the front and rear walls of the buildings. The 10-msec simulation required 15 hours on the supercomputer. The results of the two-building simulation were compared against a baseline model, in which only the second building was present to accentuate the effects of blast wave interaction with a group of buildings. All the simulations took advantage of a symmetry plane through the centre of the two buildings and the hemispherical charge that effectively reduces the model size by a factor of two.

Visualisation of pressure contours available during the post-processing stage allows a better understanding of the complex process of blast pressure interaction with a group of buildings. Figure 11 shows the blast pressure contours at the ground level 0.792 msec after detonation.

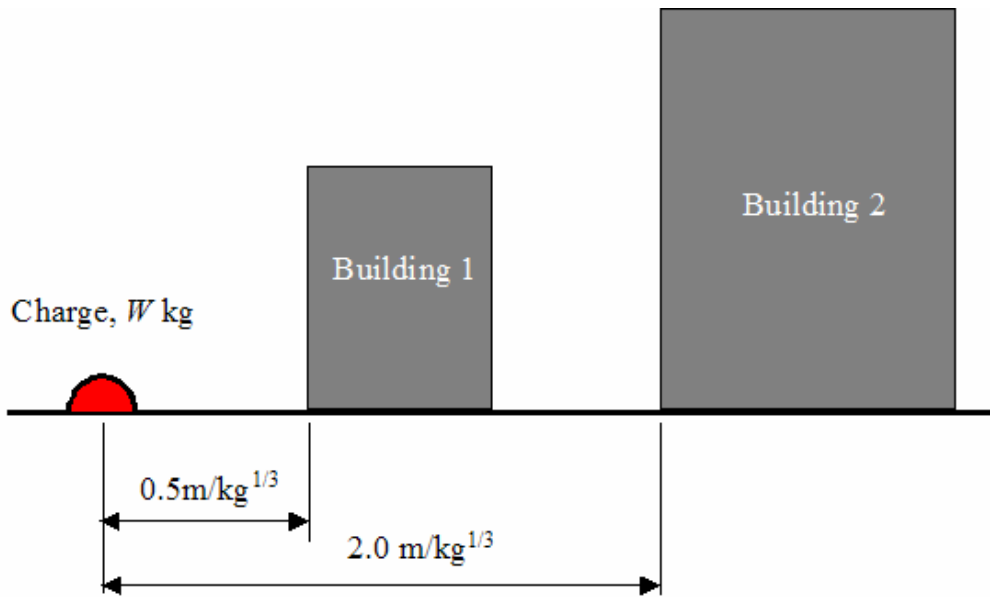


Figure 10: Two-building model showing charge location

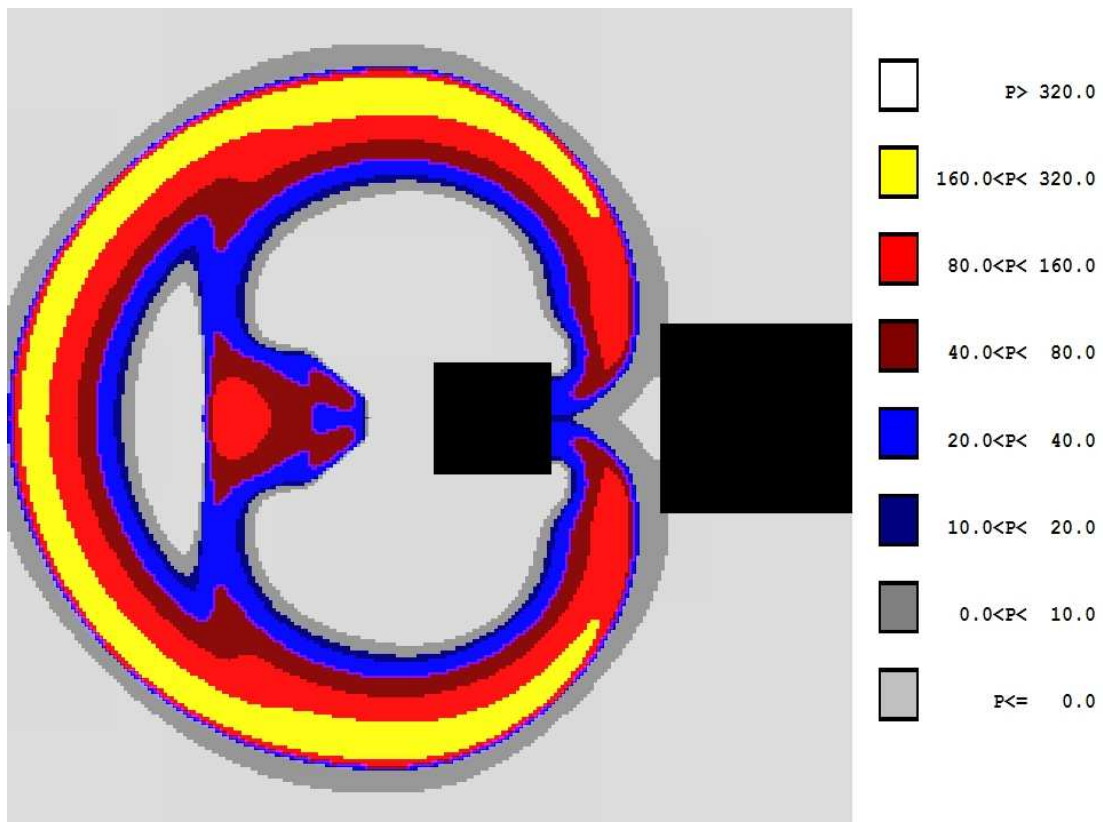


Figure 11: Blast pressure contours after $t = 0.792$ msec

By this time, blast pressures have wrapped around the corners of the front wall of Building 1, moved down the side wall, and wrapped around the rear wall of the first building. The shocks travel around the opposite sides of Building 1 and meet near the centre before reaching

Building 2. By 1.27 msec after detonation, the airblast pressure has reflected off the front wall of the back building as seen in Figure 12. At 1.93 msec after detonation, the airblast pressure has reflected on the rear wall of the first building as a result of the shock reflecting off the second building and propagating back to the rear wall of the first building.

The pressure and impulse histories measured at the ground level on the rear wall of the first building are shown in Figure 13. This figure shows that the rear wall experienced the second shock, which is about two and a half times as high as the pressure and impulse that initially loaded the building. These results clearly indicate the importance of considering adjacent structures for numerical simulation of the blast loads on buildings in an urban environment. If the presence of the second building were neglected, this would lead to a significant underestimation of the blast loads on the rear wall of Building 1. The pressure and impulse histories in Figure 13 are normalised by the peak pressure and peak positive impulse, respectively, associated with the first pressure pulse.

The relative values of the positive phase and negative phase impulses are also shown in Figure 13. The comparison of the impulses demonstrates that the negative phase impulse is three times greater than the positive phase impulse delivered by the first shock on the rear of Building 1, and twice as much as the positive phase impulse delivered by the second shock. This observation supports an assumption that the negative phase of the blast pulse may have an important influence on lightweight façade panel behaviour by causing the façade material to fail outward.

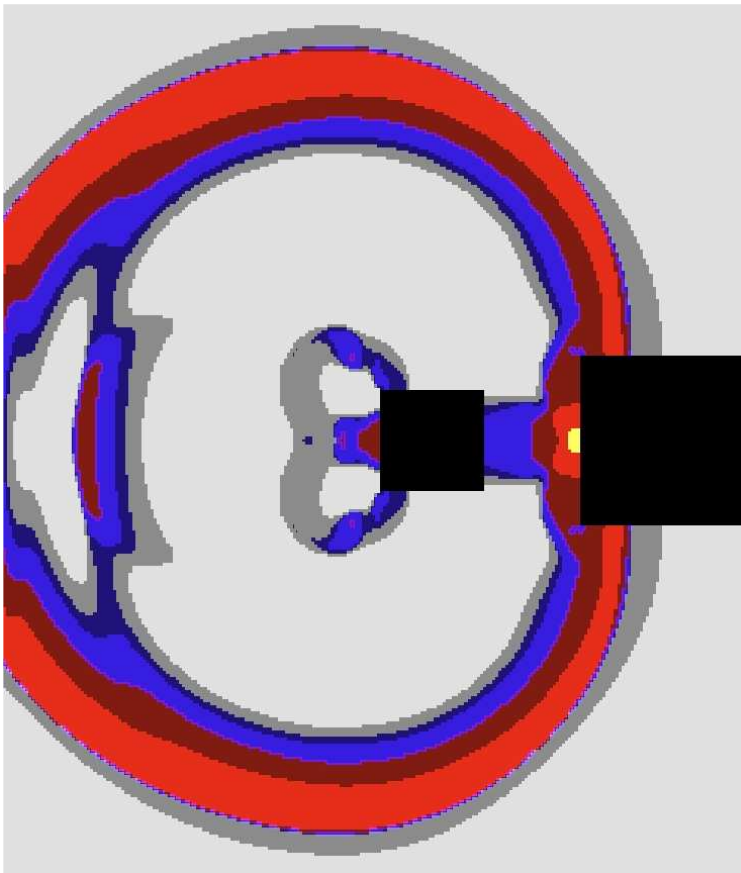


Figure 12: Blast pressure contours after $t = 1.27$ msec

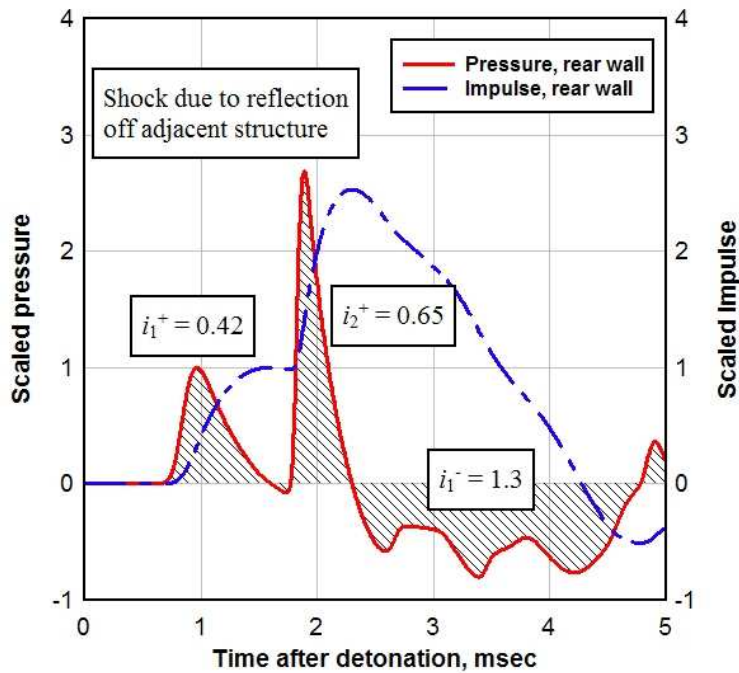


Figure 13: Blast pressure and impulse histories on rear wall of Building 1

Figure 14 shows the pressure and impulse histories at the ground level on the front wall of Building 2. The results at this location for the two-building simulation are compared to the pressure and impulse at the same point for the single building simulation, where the first structure was removed from the model, thus exposing the second building to the direct blast effects from the explosion. Pressures and impulses in Figure 14 are scaled by the peak pressure and peak positive phase impulse, accordingly, associated with the two-building model. Thus, the peak reflected pressure on the front wall of Building 2 would be overestimated by a factor of 3.5 if the building in front of it were not present. The same is true for the peak positive phase impulse, which would be over-predicted by a factor of 2.6.

Blast damage estimation using GIS technology

The results of blast simulations will be used to evaluate the degree of damage to the structure and survivability for occupants of buildings. In order to estimate damage to an individual building, blast damage to its structural components should be estimated first. Damage to individual elements is estimated based on methods of plastic analysis, structural dynamics and available experimental data for calibration [11]. Individual components are idealized as single-degree-of-freedom (SDOF) systems and their response in flexure, shear or buckling to blast loads is used to characterize the component damage. The component damage results for different construction materials (usually, steel and concrete) are typically represented by means of pressure-impulse diagrams, or P-I diagrams that define the pressure and impulse thresholds for different damage states.

After quantifying damage to individual components, the damage for the entire structure can be obtained as a weighted average of damage across different components. Some approaches of combining component damage into overall structural damage have been presented in the literature [11], but more detailed study is required to validate and improve the existing methodologies by means of data from historical blasts in urban areas.

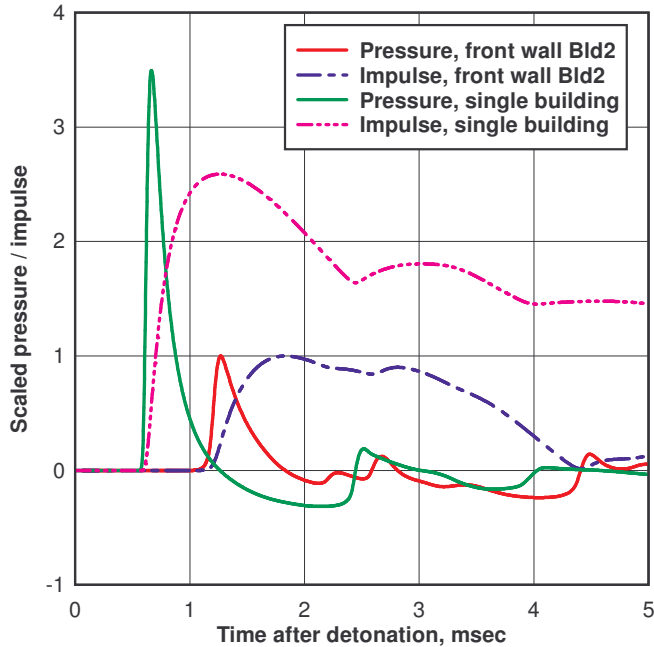
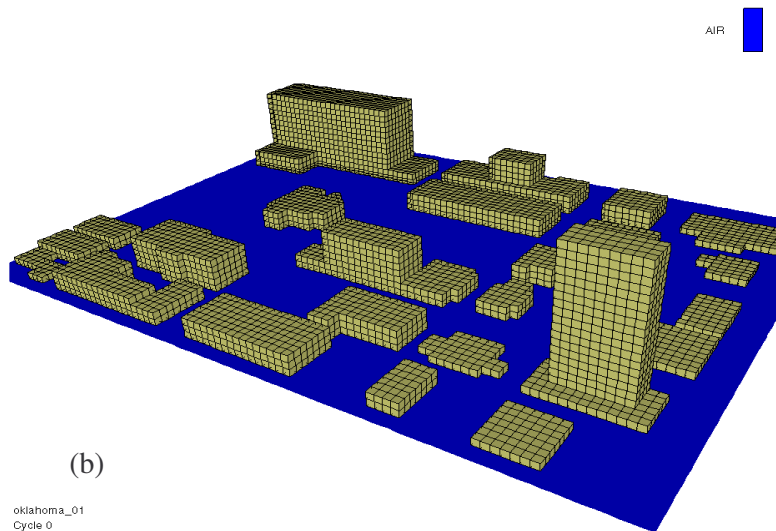


Figure 14: Comparison of pressure/impulse histories on front wall of Building 2 for single- and two-building simulations

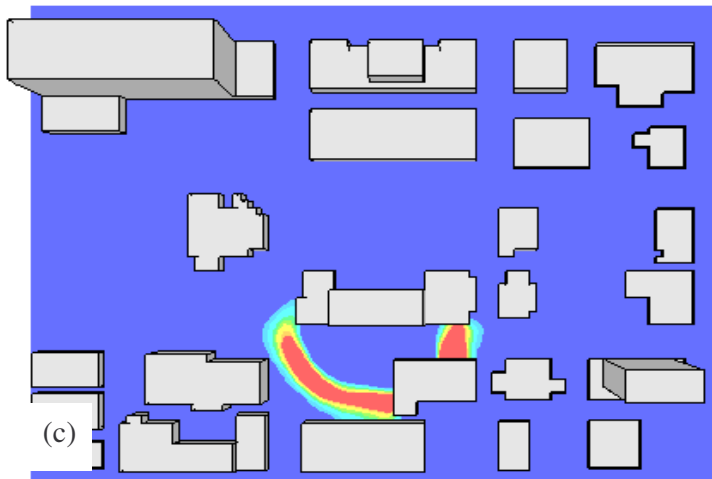
New technology is currently under development that will allow the Geographic Information System (GIS) data to be converted into computational physical domain for simulating blast effects in an urban environment. The current approach is based on manual extraction of the spatial information from the GIS database and converting it into a format suitable for incorporation in the computer models. The current approach is very time consuming. Development of a new automated interface between the GIS database and the computer model is currently under development at UoW. Figure 15 presents an example of handling the GIS datasets for the 1995 Oklahoma City bombing numerical simulations.





(b)

oklahoma_01
 Cycle 0
 Time 0.000E+000 ms
 Units m, kg, ms



(c)

Figure 15: (a) GIS data set for the Oklahoma City; (b) 3-D computer model for blast simulation; and (c) blast wave interaction with the building.

Summary

In response to a potential threat of terrorist bombings against civilian targets, various defence agencies and research organisations are examining analysis and design methodologies for mitigating the effects of a terrorist attack and improving multi-hazard building performance. Civil engineers today need guidance on how to design structural systems to withstand various acts of terrorism and threats. Better understanding of what an explosion is and how it can affect structural performance of a building are necessary for developing physical security methods. In this paper, some of the fundamental concepts of weapons effects and blast loading on a building and its components are outlined.

Some of the currently available analytical and numerical techniques that can be employed to effectively predict loads on structures when a terrorist weapon is detonated in urban environment have been discussed. It has been shown that simplified analytical techniques can be used as an engineering tool for obtaining conservative estimates of the blast effects on

buildings. Numerical techniques including Lagrangian, Eulerian, Euler-FCT, ALE, and finite element modelling should be used for accurate prediction of blast loads on commercial and public buildings.

The existing engineering-level techniques for calculating the blast effects on buildings are based on the assumption that the building experiences a load estimated assuming that it is isolated in an open space. Historical evidences suggest that the actual blast loads can either be reduced due to shadowing by intervening buildings or can be enhanced due to the presence of other buildings in the vicinity. The presented results for the two-building simulation and their comparison to the simplified methods of evaluating loads on buildings have demonstrated the importance of accounting for adjacent structures when determining the blast loads on buildings in an urban layout.

The use of both analytical techniques and sophisticated CFD numerical simulations can provide an effective approach to determining blast loads in an urban environment. Further efforts are needed to perform quantitative analysis of the phenomena of blast wave interaction with groups of structures using high performance computing facilities and massively parallel processors. This will lead to improved models for predicting blast effects as well as direct and collateral damage when a structure is subjected to a bomb attack in city centres.

References

Rose T.A and Smith P.D. (2002), "Influence of the principal geometrical parameters of straight city streets on positive and negative phase blast wave impulses", *International Journal of Impact Engineering*, 27, pp. 359-376.

Remennikov A.M. (2004), "Evaluation of blast loads on buildings in urban environment", *Proceedings of The 8th International Conference on Structures Under Shock and Impact*, pp. 73-82.

Remennikov A.M. and Rose T.A. (2005), "Modelling blast loads on buildings in complex city geometries", *International Journal of Computers and Structures*, Vol. 83, pp. 2197-2205.

U.S. Department of Army Technical Manual (TM5-1300). Design of structures to resist the effects of accidental explosions. Washington, D.C.; 1990.

Mays G.C. and Smith P.D. Blast effects on buildings: Thomas Telford; 1995.

U.S. Department of the Army, Fundamentals of Protective Design for Conventional Weapons, Technical Manual 5-855-1, 1986.

Hyde D., "User's Guide for Microcomputer Programs CONWEP and FUNPRO – Applications of TM 5-855-1", U.S. Army Engineer Waterways Experimental Station, Vicksburg, 1988.

Kingery C.N. and Bulmash G., "Airblast Parameters from TNT Spherical Air Burst and Hemispherical Surface Burst", Report ARBL-TR-02555, U.S. Army BRL, Aberdeen Proving Ground, MD, 1984.

Smith P.D., Whalen G.P., Feng L.J., et al. (2001), "Blast loading on buildings from explosions in City Streets", *Proceedings of the Institution of Civil Engineers-Structures & Buildings*, 146(1), pp.47-55.

Rose T.A. Air3D User's Guide. 7.0: RMCS, Cranfield University, UK; 2003.

FACEDAP: Facility and component explosive damage assessment program, Theory Manual, Version 1.2, 1994.